Ecological Indicators 90 (2018) 426–437

Contents lists available at ScienceDirect

Ecological Indicators

journal homepage: www.elsevier.com/locate/ecolind

Spatiotemporal changes and drivers of global land vegetation oxygen production between 2001 and 2010

Lijuan Zhang[a,*], Bingyan Zhang[a], Wenliang Li[b], Xiaxiang Li[a], Li Sun[a], Lanqi Jiang[c], Xiaoxue Liu[a]

[a] Key Laboratory of Remote Sensing Monitoring of Geographic Environment, College of Heilongjiang Province, Harbin Normal University, No. 1 South Shida Road, Limin Economic Development Zone, Harbin, Heilongjiang 150025, China
[b] Department of Geological and Atmospheric Science, Iowa State University, Ames, IA 50010, USA
[c] Innovation and Opening Laboratory of Regional Eco-Meteorology in Northeast, China Meteorological Administration, Meteorological Academician Workstation of Heilongjiang Province, Heilongjiang Province Institute of Meteorological Sciences, Harbin 150030, China

ARTICLE INFO

Keywords:
Land vegetation
Oxygen production
Spatiotemporal variations
Influencing factors
Global change

ABSTRACT

Oxygen is a sensitive indicator of atmospheric compositional changes, and also a primary requirement for human life. Values for the normalized difference vegetation index (NDVI), temperature, and radiation are input into the C-FIX model in this study in order to simulate global net ecosystem productivity (NEP). According to carbon–oxygen equilibrium theory, NEP is further converted into oxygen production by land vegetation around the world. Thus, an in-depth analysis of spatiotemporal changes in the oxygen production of land vegetation globally is presented in this study alongside a discussion of relevant mechanisms of change. The results of this research show that global annual average oxygen production between 2001 and 2010 had a significant increasing trend, amounting to 194×10^{10} t, at a rate of 0.78×10^{9} t/a. Data show that the most obvious increases in oxygen production occurred in Asia, Europe, and North America, while changes in Africa, South America, and Oceania were insignificant. Global maximum oxygen production was seen in South America, encompassing roughly 30% of the global total, while between 2001 and 2010, the distribution of production by global land vegetation can be characterized by a gradual decrease from the equator to the poles. Production on approximately 12.0% of global landmass increased significantly (mainly in eastern Siberia, eastern Europe, and in the western part of North America), while a significant decrease was observed on approximately 5.43% of global landmass (mainly in western Siberia, central Africa, and the southern part of South America). At the same time, changes in carbon dioxide (CO_2) concentration and vegetation resulted in an overall increase in global oxygen production, while climate change led to a decrease. Moreover, the increase of CO_2 concentration is the main factor for the significant increase in the total oxygen production of land vegetation in the world, accounting for 70.0%, while the conversion of cultivated land and grassland into forested land led to significant global decreases. The main contributions of this study are thus to reveal the spatial distribution of, and variation in, global oxygen production by vegetation over the last decade, and to clarify the factors that have influenced these changes.

1. Introduction

Climate warming-related changes in atmospheric carbon dioxide (CO_2) content have attracted worldwide attention. However, another change in atmospheric chemical composition, a gradual reduction in oxygen (O_2), has been largely ignored, even though it directly threatens all life on Earth. Measurement data suggest that the oxygen content of the lower atmosphere has gradually decreased over time, at a rate of 2 ppm/year (Santilli, 2000), while in some heavily polluted cities and industrial regions where population density is relatively large, oxygen content is around 15.0% or lower (Santilli, 2000; Lenton, 2003). A lowered atmospheric oxygen content (i.e. less than 19.5%) creates symptoms of anoxia, a direct cause of cell hypoxia which leads to chronic pain and diseases (Semenza, 2001; Jacobsen, 2008).

The majority of atmospheric oxygen is the result of photosynthesis by algae in oceans and green plants on land (Kasting and Siefert, 2002; Schäfer, 2004). In recent years, however, because of intensifying human activity, great changes in land use and land cover (LUCC) have taken place around the world (Foley et al., 2005; Grimm et al., 2008; Friedl et al., 2010). Forested area, for example, decreased by 1,500,000 km^2 between 2000 and 2012 (Hansen et al., 2013), being mainly converted into either cultivated land or grassland (Zak et al., 2008; Tsegaye et al., 2010). Changes in both the area and quality of vegetation affect photosynthetic intensity as well as global oxygen

* Corresponding author.
E-mail address: zlj19650205@163.com (L. Zhang).

https://doi.org/10.1016/j.ecolind.2018.03.041
Received 24 August 2017; Received in revised form 1 February 2018; Accepted 17 March 2018
Available online 21 March 2018
1470-160X/

production, while temperature changes influence enzyme activity during this process. The 5th Report of the Intergovernmental Panel on Climate Change (IPCC) noted that, from the mid-19th century onwards, when observations started, global average temperature has risen by about 0.8 °C. The period between 1983 and 2012 probably experienced the highest temperatures seen over the last 1400 years, and levels are expected to further increase (IPCC, 2013). At the same time, CO_2 is a key resource for photosynthesis and the concentration of this gas in the atmosphere continues to increase; atmospheric CO_2 concentration has increased by nearly 30.0% since the early stages of the Industrial Revolution, and the annual average increase per year over the last ten years has been between 1 ppmv and 3 ppmv (Tao et al., 2001). Thus, in the context of increasing global LUCC intensity and speed, as well as continuously increasing temperature and CO_2 concentration, evaluating changes in global oxygen production remains a key scientific problem worthy of further discussion, not least because this gas is essential to all organisms on Earth. The ever increasing levels of global environmental pollution weaken the strength and intensity of solar radiation; as illumination intensity influences photosynthesis via photochemical reactions, the issue of global oxygen production is even more significant and urgent.

The photosynthesis of green plants both produces organic matter ($C_6H_{12}O_6$) and oxygen and consumes a part of them via respiration. Three basic measures of the carbon (C) cycle, gross primary productivity (GPP), net primary productivity (NPP), and net ecosystem productivity (NEP), have been defined in the literature (Tao et al., 2001), and according to the principles of photosynthesis and respiration, a proportional relationship exists between the organic C (OC) and oxygen absorbed and released by vegetation. This means that the amount of oxygen produced by vegetation can be estimated via the volume of OC, an approach referred to as the carbon–oxygen equilibrium method. A review of relevant literature reveals that a number of previous researchers have estimated oxygen production using GPP (Zhang et al., 2007; Chen and Lu, 2009), while others have utilized NPP (Peng, 2003; Ma et al., 2011). The first of these measures, GPP, incorporates the initial OC produced via photosynthesis without taking into account the amount consumed by vegetation respiration, while the second, NPP, considers the OC that remains after accounting for plant autotrophic respiration. However, as NPP does not take into account the OC consumed via plant heterotrophic respiration, results based on these different measures can be different from one another. Distinct from the GPP and NPP, the NEP takes into account OC that remains after both autotrophic and heterotrophic respiration (Zhang et al., 2014; Liu et al., 2015); in other words, this measure refers to net photosynthetic production after respiration. It is clear, therefore, that estimates based on NEP represent net oxygen production and so more directly evaluate both the change and content of this gas in the atmosphere. Surprisingly, however, no research to date has been conducted to evaluate the global oxygen production of vegetation based on the NEP.

The aim of the study is to simulate the global annual oxygen production of vegetation between 2001 and 2010 using the photosynthetic light energy utilization (C-FIX) model. This was achieved by simulating the global NEP of land vegetation, and then converting these values into oxygen production based on photosynthesis and respiration equations. The goal of this research is therefore to explore spatiotemporal changes in the global oxygen production of vegetation, as well as the factors that have influenced variation. The main contribution of this study is to reveal the oxygen content of the atmosphere produced by land plant photosynthesis over the last ten years, as well as to discuss its variation, and reveal the factors that contribute to change. The results of this study thus provide a quantitative baseline for research on global atmospheric oxygen content changes as well as environmental assessment.

2. Data

The data sources as well as the steps taken to process the three major parameters of the C-FIX model are discussed in this section. The three parameters that comprise this model are the normalized difference vegetation index (NDVI), daily average temperature, and daily average radiation.

2.1. The NDVI

The NDVI, the most appropriate indicator for vegetation growth status and coverage, is equivalent to an index change in biomass, which is calculated as follows (Running et al., 2000):

$$NDVI = \frac{NIR - Red}{NIR + Red} \quad (1)$$

where *NIR* and *Red* denote the reflectance values of the near-infrared and red bands, respectively. As this index is calculated based on these two bands, it also relies on an atmospheric correction; thus, when there are no clouds or snow, as well as a relatively low aerosol content, NDVI values are very precise. This index reflects vegetation status, but is also affected by the plant canopy background factors, including soils, humid ground, snow, dead leaves, and surface roughness. For example, if a surface is very bright or dark, such as the case for snow, desert oases, or inland water bodies, NDVI values are not stable; thus, to minimize calculation error, NDVI data was processed in this study according to the steps. In cases where the NDVI is negative, the land surface is covered by clouds, water, or snow, but if the index is zero, then the land surface is covered by construction land, rock, or barren land in place of vegetation. However, if the NDVI is positive, then the land surface is covered with vegetation; this coverage increases with the increase of the index values. As the aim of this study is to evaluate vegetation oxygen production, negative NDVI values are inconsistent with simulation conditions; thus, during calculations, oxygen production is marked as zero in areas where the NDVI is negative.

NDVI was obtained from the NASA MOD13A2 product via the Terra satellite platform at a spatial resolution of 1 km × 1 km and a temporal resolution of 16 days, and 6690 images were collected to cover the global regions (https://ladsweb. nascom. nasa.gov). The NDVI data used in this study covered the period between January 1st, 2001, and December 31st, 2010, and a total of 66,900 images were collected. Image format conversion and mosaics were conducted using ERDAS9.2, with resolution reset as 0.5° using MATLAB. Global regional image cutting, superposition, and meaning were performed using ArcGIS; during these steps, if two images were available for a given month, then the average of the two was used; the final data set comprised a total of 120 grid image layers of monthly NDVI values between 2001 and 2010 at a spatial resolution of 0.5° × 0.5°. In particular, each of the 0.5° × 0.5° grids included 3080 grids that had a spatial resolution of 1 km × 1 km such that resolution increased to 0.5° from 1 km. An average value of the 3080 child grids was chosen as the NDVI for the parent grid.

2.2. Daily average temperature

The C-FIX model provides a daily simulation that requires temperature input. However, because of the extensive calculations required by this study, monthly rather than daily average values were used. Monthly average temperatures for the period between 2001 and 2010 were extracted from the Climate Research Institute (CRU) (University of East Anglia, Norwich, UK) CRU-TS3.2.4.1 data set, in the form of global regional values downloaded from the website (http://www.cru.uea.ac.uk/cru/data) using a program created using FORTRAN. These data were then converted into a grid format using the “To Raster” tool in the Spatial Analyst Tools model within ArcGIS. A total of 120 image layers for monthly average gridded temperature data between 2001 and 2010

were obtained, at a spatial resolution of 0.5° × 0.5°.

2.3. Daily ground radiation

Ground radiation flux was estimated in this study using astronomical radiation and cloud cover, as proposed by Kimball (1928). This estimation method was considered applicable to data across all regions, and was calculated as follows:

$$S_{g,d} = S_{o,d}(0.29 + 0.71(1.0-C)) \quad (2)$$

where $S_{g,d}$ denotes daily incoming global solar radiation (MJ/m^2/d), $S_{o,d}$ is the daily extraterrestrial radiation (MJ/m^2/d), and C denotes mean total cloud cover during the daytime. The formula for $S_{o,d}$ used in this study follows Zhou et al. (2003), as follows:

$$S_{o,d} = \frac{T}{\pi}\frac{I_0}{\rho^2}(\omega_0 \sin\varphi \sin\delta + \cos\varphi \cos\delta \sin\omega_0) \quad (3)$$

where T/π is 458.4, I_0 refers to the solar constant (W/m^2), ρ denotes the daily mean distance correction term, ω_0 is the solar hour angle (°), φ is latitude (rad), and δ is the solar declination (rad).

The monthly average cloud cover values used in this study were also extracted from the CRU-TS3.2.4.1 data set, and were processed in the same way as described above for daily average temperature data. Thus, a total of 120 image layers for monthly average cloud cover for the period between 2001 and 2010 were downloaded at a spatial resolution of 0.5° × 0.5°, and astronomical radiation was calculated using Eq. (3) and the ArcGIS grid calculation method. The ω_0, φ, and δ of each grid were input into Eq. (3), while monthly average ground radiation was calculated using Eq. (2). A total of 120 image layers for monthly average ground radiation for the period between 2001 and 2010 were obtained at a spatial resolution of 0.5° × 0.5°.

2.4. Land usage data

The light utilization efficiency (ε) included in the C-FIX model refers to the efficiency of plants with respect to GPP. A review of the relevant literature suggests that the most appropriate value for this parameter is 1.10 g C/MJ (APAR) (Veroustraete et al., 2002; Lu et al., 2004; Verstraeten et al., 2006). However, as different plants have different ε levels, a range of values were incorporated in this study based on previous research results (Table 1) (Peng et al., 2000; Running et al., 2000; Zhu et al., 2004, 2006). Annual global land use and land cover data for the period between 2001 and 2010 were collected from MCD12Q1 (https://ladsweb.nascom.nasa.gov), a Terra and Aqua synthetic satellite product also provided by NASA at a spatial resolution of 500 m × 500 m, and a temporal resolution of one year comprising 317 images. Image format conversion and mosaics were processed using ERDAS9.2, image resolution was reset to 0.5° using MATLAB, and global regional image cutting and data extraction were performed using ArcGIS. A total of ten image layers for annual global land use and land cover encompassing the period between 2001 and 2010 were downloaded with a grid resolution of 0.5° × 0.5°. Each of these cells included 12,321 child grids with a 500 m × 500 m spatial resolution when overall resolution was increased to 0.5° from 500 m; thus, the child grid containing the largest proportion was selected as the land use and land cover type for a parent. On the basis of different plant ε values (Table 1), data for particular plants within the 0.5° × 0.5° grids were determined using global land use and land cover images for the period between 2001 and 2010.

Table 1
Light utilization efficiency (ε) of vegetation in different land use types.

Land use types	Value (gC/MJ)	Land use types	Value (gC/MJ)
Evergreen coniferous forest	1.01	Dense shrubs & Sparse shrubs	0.83
Evergreen broad-leaved forest	1.26	Savanna	0.77
Deciduous coniferous forest	1.10	Grassland	0.61
Deciduous broad-leaved forest	1.04	Cultivated land	0.60
Mixed forest	1.12	Sparse Vegetation	0.39
Construction land	0.39	Wetland & Shore	0.39

3. Research methods

3.1. The C-FIX model

The C-FIX model was used to simulate NEP. As discussed, this approach comprises a light-energy utilization ratio model that is based on Monteith theory and can be used to estimate the productivity (i.e. GPP, NPP, and NEP) at either global or regional scales (Veroustraete et al., 2002). The advantages of the C-FIX model include a small number of parameter inputs, a high calculation efficiency, and enhanced output result spatiotemporal resolution (Lu et al., 2005; Zhang et al., 2014). This approach, which is therefore both effective and practical (Zhang et al., 2014; Liu et al., 2015), has been widely applied in recent years both domestically and internationally to calculate vegetation productivity, and has generated good simulation results (Veroustraete et al., 2002; Lu et al., 2005; Chen et al., 2007; Zhang et al., 2011, 2014; Liu et al., 2015). The formulae embedded within the C-FIX model that are used to calculate daily GPP, NPP, and NEP values for a given grid are as follows:

$$GPP_d = p(T_{atm}) \times CO_2 fert \times \varepsilon \times fAPAR \times c \times S_{g,d} \quad (4)$$

$$NPP_d = GPP_d \times (1-A_d) \quad (5)$$

$$NEP_d = NPP_d - R_{h,d} \quad (6)$$

$$p(T_{atm}) = \frac{e^{\left(C_1 - \frac{\Delta H_{a,p}}{Rg \cdot T}\right)}}{1 + e^{\left(\frac{\Delta S \cdot T - \Delta H_{d,p}}{Rg \cdot T}\right)}} \quad (7)$$

$$CO_2 fert = \frac{[CO_2] - \frac{[O_2]}{2\tau}}{[CO_2]^{ref} - \frac{[O_2]}{2\tau}} \frac{K_m(1 + \frac{[O_2]}{K_0}) + [CO_2]^{ref}}{K_m(1 + \frac{[O_2]}{K_0}) + [CO_2]} \quad (8)$$

$$fAPAR = 1.1638 \times NDVI - 0.1426 \quad (9)$$

$$A_d = (7.825 + 1.145T_a)/100 \quad (10)$$

$$R_{h,d} = k_{s,y} \cdot Q_{10}^{T_a/10} \quad (11)$$

The units of GPP, NPP, and NEP are g C/m^2/d in these expressions, and use of the subscript d denotes daily values.

The parameters in Eqs. (4)–(11) are listed in Table 2; some required additional calculations, while some were obtained directly (Veroustraete et al., 2002; Verstraeten et al., 2006).

Values for K_m, K_0, τ, and $K_{s,y}$ were calculated as follows:

$$K_m = Ae^{(-E_a/R_g T)} \quad (12)$$

Thus, applying Eq. (12), if $T \geq 15$ °C (288.15 K) then $E_{a1} = 59.4$ kJ/mol and $A_1 = 2.419 \times 10^{13}$, or if $T < 15$ °C (288.15 K) then $E_{a2} = 109.6$ kJ/mol and $A_2 = 1.976 \times 10^{22}$.

The inhibition constant (K_0) for O_2 was calculated using Eq. (12), such that $A_0 = 8240$ [%O_2] and $E_{a0} = 13.9135$ kJ/mol. Thus, the CO_2/O_2 specificity ratio τ is calculated as follows:

$$\tau = A_\tau e^{(-E_{a\tau}/R_g T)} \quad (13)$$

where $A_\tau = 7.87 \times 10^{-5}$, and $E_{a\tau} = -42.8969$ kJ/mol. Thus:

Table 2
Description of parameters in the C-FIX model.

Parameter	Significance	Value	Unit	Parameter	Significance	Value	Unit
$p(T_{atm})$	Normalised temperature dependency factor	[0,1]		ΔS	Entropy of the denaturation equilibrium of CO_2	704.98	J/K/mol
CO_2fert	Normalised CO_2 fertilisation factor			R_g	Gas constant	8.31	J/K/mol
ε	Radiation Use Efficiency (RUE)	1.10	gC/MJ (APAR)	$[CO_2]$	Currently determined concentration of atmospheric CO_2		mg/m^3
$_C$	Climatic efficiency	0.48		$[O_2]$	Currently determined concentration of atmospheric O_2	20.9	mg/m^3
$S_{g,d}$	Daily incoming global solar radiation		$MJ/m^2/d$	τ	CO_2/O_2 specificity ratio		
A_d	Autotrophic respiratory fraction			K_m	Affinity constant for CO_2 of Rubisco		$[\%CO_2]$
$R_{h,d}$	Heterotrophic respiration		$gC/m^2/d$	K_0	Inhibition constant for O_2		$[\%O_2]$
C_1	Constant	21.77		$[CO_2]^{ref}$	Mixed concentration of CO_2 in the atmospheric background level	285	mg/m^3
$\Delta H_{a,p}$	Activation energy	52,750	J/mol	*NDVI*	Normalized Difference Vegetation Index		
$\Delta H_{d,p}$	Deactivation energy	211,000	J/mol	T_a	Atmospheric temperature		°C
T	Air temperature		K	$k_{s,y}$	Heterotrophic respiratory rate coefficient		$gC/m^2/d$
fAPAR	Fraction of absorbed Photosynthetically Active Radiation (PAR)	[0,1]		Q_{10}	The relative increase of the respiratory flux for a 10 °C increase in temperature	1.5	

$$k_{s,y} = \frac{\sum_{d=1}^{365} \frac{GPP_d}{b_y}}{\sum_{d=1}^{365} p(T_{atm})_d} \quad (14)$$

where b_y denotes the annual average calibration coefficient of soil heterotrophic respiration and has a value of 1.0.

3.2. Estimating land vegetation net oxygen production

Photosynthesis is the process in which chlorophyll transforms CO_2 and water (H_2O) into $C_6H_{12}O_6$ and O_2 in the presence of sunlight (Lenton, 2003). The formula for photosynthesis is as follows:

$$6CO_2 + 6H_2 \xrightarrow{sunshine} C_6H_{12}O_6 + 6O_2 \quad (15)$$

Green plants produce OC via photosynthesis; the amount produced per unit area and time is referred to as primary productivity (GPP). At the same time, however, green plants also consume $C_6H_{12}O_6$ and O_2, and release CO_2 via respiration. The formula for respiration is as follows (Lenton, 2003):

$$C_6H_{12}O_6 + 6O_2 \rightarrow 6CO_2 + 6H_2O \quad (16)$$

The OC that remains after taking autotrophic respiration into account is referred to as NPP, while the OC that remains after accounting for both autotrophic and heterotrophic respiration is referred to as NEP which is calculated via the oxygen production of plants, using a value of 1:2.67 in Eq. (15). Thus, daily oxygen production was calculated first so that a monthly value could be estimated by multiplication, and an annual value could be calculated by summation.

3.3. Controlled experiments

A series of three controlled experiments were designed to explore the factors driving changes in global oxygen production. Thus, the oxygen production of plants under different scenarios was simulated in the presence of controlled driving factors and further compared to actual gas production values, while the effects of the NDVI, atmospheric CO_2 concentration, and climate on plant oxygen production were analyzed quantitatively (Table 3).

The first controlled experiment addressed the effects of vegetation change on oxygen production. This scenario assumed that global climate and CO_2 concentration in the atmosphere between 2001 and 2010 remained constant, and NEP was simulated by driving the C-FIX model using 2001 temperature, radiation, and CO_2 concentration and the 2010 NDVI value. Values for oxygen production were estimated in this experiment; thus, the difference between experimental and actual values for 2001 reflects the quantitative change in the production of this gas resulting from vegetation change. The formula for this is as follows:

$$\Delta_{variation} = O_{2,\text{control}} - O_{2,2001} \quad (17)$$

where $\Delta_{variation}$ denotes the change in global oxygen production, $O_{2,control}$ denotes estimated oxygen production in the controlled experiment, and $O_{2,2001}$ is the actual value of global oxygen production in 2001. In order to ensure comparative accuracy between estimation results and to reduce the impact of abnormal fluctuations, temperatures for 2001 and 2010 were also substituted with averages from 2001 to 2003 and from 2008 to 2010, respectively.

3.4. Analysis of spatial similarities

In order to determine the level of similarity between spatial distribution maps of global land vegetation oxygen production for the period between 2001 and 2010, the Kappa Index was applied to determine the consistency of different models and methods of analysis. Coefficients of the Kappa Index range between 0 and 1 such that different amounts of similarity are represented by five groups of values. Thus, values between 0 and 0.20 denote extremely low consistency, while values between 0.21 and 0.40 denote low consistency, values between 0.41 and 0.60 denote a medium-level of consistency, values between 0.61 and 0.80 denote high consistency, and values between 0.81 and 1 denote extremely high consistency (Viera and Garrett, 2005).

Table 3
Controlled experiments.

Controlled experiments	Year		Simulated results	$\Delta_{variation}$	Significance
	2010	2001			
Controlled experiment 1	*NDVI*	T_a; $S_{g,d}$; $[CO_2]$	$O_{2,control1}$	$O_{2,control1}-O_{2,2001}$	Changes caused by vegetation
Controlled experiment 2	$[CO_2]$	T_a; $S_{g,d}$; *NDVI*	$O_{2,control2}$	$O_{2,control2}-O_{2,2001}$	Changes caused by atmospheric CO_2 concentration
Controlled experiment 3	T_a; $S_{g,d}$	*NDVI*; $[CO_2]$	$O_{2,control3}$	$O_{2,control3}-O_{2,2001}$	Changes caused by climate (Temperature and radiation)

Note: $O_{2,control1}$, $O_{2,control2}$, and $O_{2,control3}$ are the simulation values of the controlled experiments 1–3.

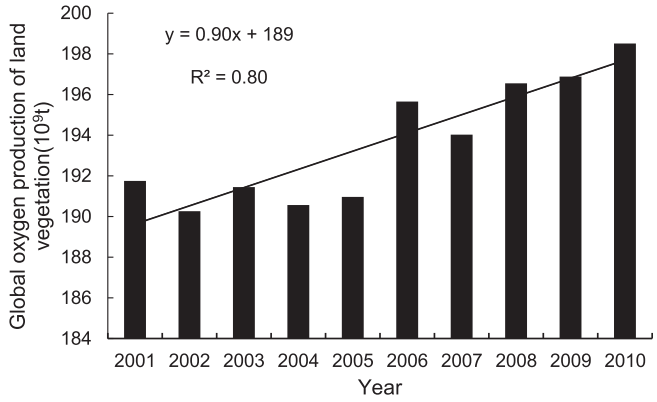

Fig. 1. Temporal changes in global oxygen production of land vegetation from 2001 to 2010.

4. Results

4.1. Temporal changes in global oxygen production

The results of this study show that global annual oxygen production between 2001 and 2010 ranged from 190×10^9 t to 199×10^9 t (average: 194×10^9 t; annual variation coefficient: 0.02). The maximum recorded value was in 2010, while the minimum was in 2002, and the difference between these values was 8.24×10^9 t. Data show that global annual oxygen production has tended to increase over time in an extremely significant manner ($P < 0.01$); the annual average increase in oxygen production over this period was 0.78×10^9 t, incorporating an obvious change around 2006. Results show that global annual oxygen production after 2006 was obviously greater than previously ($P < 0.01$) (Fig. 1).

This study shows that the oxygen production of South America ranked first amongst the continents, ranging between 53.5×10^9 t and 56.6×10^9 t, then followed by Asia, Africa, North America, and Europe. The oxygen production of Oceania was the lowest among continents, ranging between 11.3×10^9 t and 13.0×10^9 t (Fig. 2). Data show that the annual oxygen production across all the continents tended to increase between 2001 and 2010. In particular, the annual oxygen production in Asia, Europe, and North America significantly increased by 1.94×10^8 t/a, 1.61×10^8 t/a, and 1.60×10^8 t/a, respectively ($P < 0.05$). While increases in Africa, South America, and Oceania were not significant ($P > 0.05$). The oxygen production increase in Asia was the highest overall, while oxygen production per unit area was the highest in South America, 308×10 t/km^2, followed by Europe, Oceania, and Africa; oxygen production values per unit area exceeded 130×10 t/km^2 in these regions. In contrast, Asia and North America exhibited the lowest oxygen production values per unit area, both less than 110×10 t/km^2 (Table 4).

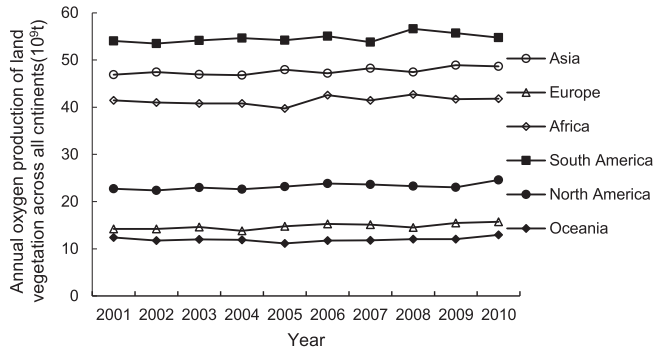

Fig. 2. Temporal changes in oxygen production of land vegetation across all continents from 2001 to 2010.

4.2. Global spatial distribution and changes in the land vegetation oxygen production

4.2.1. Spatial distribution

The spatial distribution of global oxygen production between 2001 and 2010 is shown in Fig. 3. Over this time period, annual Kappa values ranged between 0.69 and 0.84, indicative of extremely high consistency, and tended to decrease from the equator to the poles (Fig. 3). In terms of the annual oxygen production per unit area, values for tropical areas were the highest; the most elevated values were primarily in regions of Southeast Asia, including northern Myanmar, Laos, Vietnam, Indonesia, and Malaysia, as well as in central Africa, including the Democratic Republic of the Congo, in southern North America, including southeastern Mexico, Guatemala, Honduras, Nicaragua, and Costa Rica, and in northern South America, including southern Venezuela, Guyana, eastern Peru, northwestern Brazil, and eastern Bolivia. These countries and regions all had values of annual oxygen production per unit area higher than 400×10 t/km^2.

The spatial distribution of global oxygen production has changed over time. Specifically, between January and July, higher annual values of oxygen production have shifted to the Northern Hemisphere from the Southern Hemisphere, while the opposite trend has characterized the period between August and December (Fig. 4). For instance, in January, higher oxygen production values are seen in the Southern Hemisphere, primarily in South America, southern Africa, and in Southeast Asia, ranging between 200 t/km^2 and 400 t/km^2. In contrast, in July, higher oxygen production levels are seen in the Northern Hemisphere as well as in low-latitude areas around the equator, primarily central and eastern parts of North America, northern South America, central and western parts of Russia, Southeast Asia, and in most parts of Europe. In these regions, levels ranged between 400 t/km^2 and 800 t/km, while in terms of oxygen production per unit area, levels in the Northern Hemisphere in July were higher than those seen in the Southern Hemisphere in January. This difference is primarily due to plant growth periods, as summer (when plant growth is the fastest) occurs in July in the Northern Hemisphere and in January in the Southern Hemisphere. At the same time, both the vegetated area and varieties of plants seen in the Northern Hemisphere exceed those of the Southern Hemisphere; these differences also mean that oxygen production in the Northern Hemisphere in July is higher than in the Southern Hemisphere in January.

4.2.2. Spatial variations of oxygen production

The oxygen production across 52.0% of the globe tended to increase between 2001 and 2010. In particular, areas of production increase were primarily distributed in North America, eastern South America (including in Brazil and Bolivia), southern Africa (including the Democratic Republic of the Congo, Angola, Zambia, Zimbabwe, and Botswana), southern Europe, eastern Asia (including northeastern China and eastern Siberia), and eastern Australia. In contrast, oxygen production across 48.0% of the globe has tended to decrease over the study period. Areas that have experienced decreases are primarily distributed in western Siberia, southeastern China, Norway, Sweden, western Australia, Nigeria, southern Chad, southern Sudan, southern Argentina, and eastern Canada (Fig. 5). Data show in the regions abovementioned, 12.0% have experienced a significant increase ($P < 0.05$), while 5.43% have experienced a significant decrease ($P < 0.05$), together encompassing roughly 17.0% of the globe. In other words, areas that have seen either a significant increase or decrease in oxygen production cover approximately one-fifth of the globe. Specifically, the global area with a significant increase is approximately twice that with a significant decrease. Areas that have seen significant increases in oxygen production are mainly distributed in eastern Siberia, eastern Europe, northeastern China, eastern Australia, southern Africa, eastern South America, Mexico, central America, and the border region between Alaska and Canada, while areas that have experienced significant

Table 4
Changes in oxygen production of land vegetation across all continents.

Continents	Annual total (10^9 t)	Amount per unit area ($\times 10$ t/km^2)	Variation (10^9 t)	Change rate (%)	Increase rate (10^8 t/a)	Variation coefficient
Asia	47.7	106	1.77	3.78	1.94*	0.02
Europe	14.8	149	1.51	10.6	1.61*	0.04
Africa	41.4	138	0.35	0.85	1.37	0.02
South America	54.6	308	0.71	1.32	1.97	0.02
North America	23.2	96.0	1.86	8.16	1.60*	0.03
Oceania	12.0	147	0.56	4.52	0.47	0.04

* Passing 0.05 level probability test.

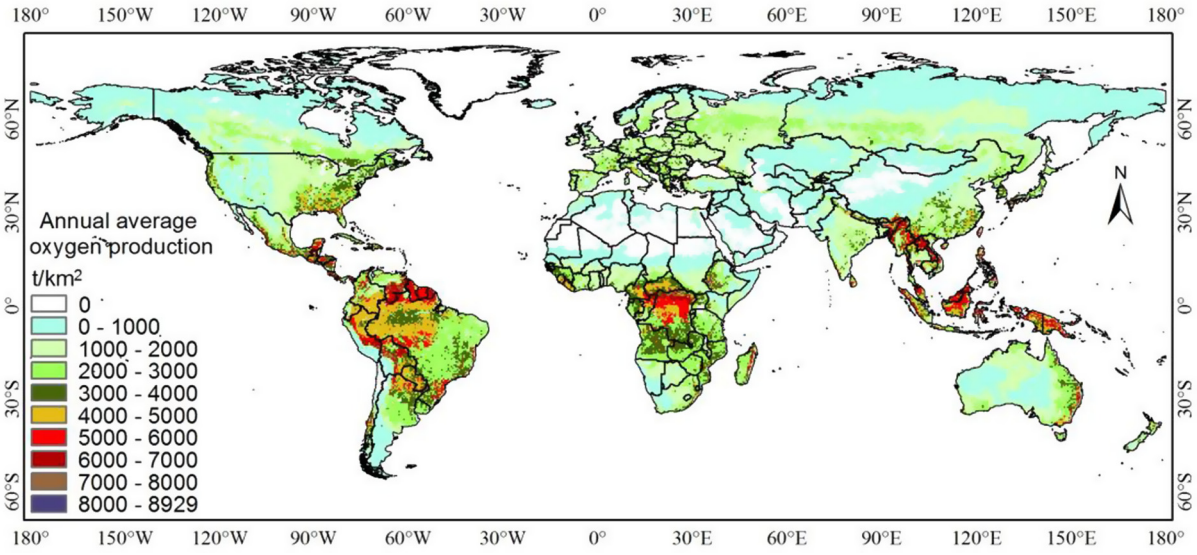

Fig. 3. Spatial distribution of annual oxygen production averaged over the period 2001–2010.

decreases are mainly found in western Siberia, central Africa, western Australia, and southern South America (Fig. 6).

4.3. Influencing factors

The results of the controlled experiments presented in this study reveal that changes in vegetation and CO_2 concentration have both resulted in increases in global oxygen production. In particular, a change in CO_2 concentration resulted in an oxygen production increase of 7.61×10^9 t, while a change in vegetation led to an increase of 2.08×10^9 t. Similarly, results suggest that climate change has resulted in an oxygen production decrease of 0.92×10^9 t (Table 5). Simulation results suggest that changes in CO_2 concentration can account for 71.7% of recorded changes in oxygen production, while variations in vegetation and climate can account for 19.6% and 8.67%, respectively. In other words, changes in atmospheric CO_2 concentration can mainly explain increases in global oxygen production.

The spatial distribution of the controlled experimental results suggest that changes in vegetation have resulted in increases, decreases, or no changes in oxygen production across 45.3%, 36.2%, and 18.5% of global area, respectively. However, 1.25 times the area has experienced increases compared to decreases, with amounts ranging between 0 t/km^2 and 500 t/km^2; these areas of increase are primarily distributed in the western and eastern parts of Russia, northeastern China, eastern Australia, the border area between Alaska and Canada, the USA, and Mexico. At the same time, decreasing amounts of oxygen production ranged between -500 t/km^2 and 0 t/km^2; areas experiencing decreases tended to be distributed in western Siberia, southeastern China, western Australia, southern Africa, and South America (Fig. 7). Results show that CO_2 concentration changes resulted in increases, decreases, or no change in oxygen production in 75.1%, 5.44%, and 19.5% of global area, respectively. This translates to a 13.8 times larger area of increasing oxygen production than decreasing; amounts of increase ranged between 0 t/km^2 and 500 t/km^2, while amounts of decrease

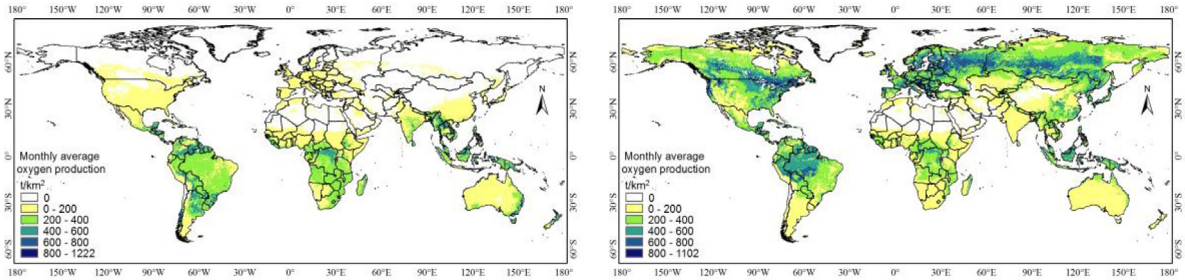

Fig. 4. Spatial distribution of monthly oxygen production averaged over the period 2001–2010 (in January and July).

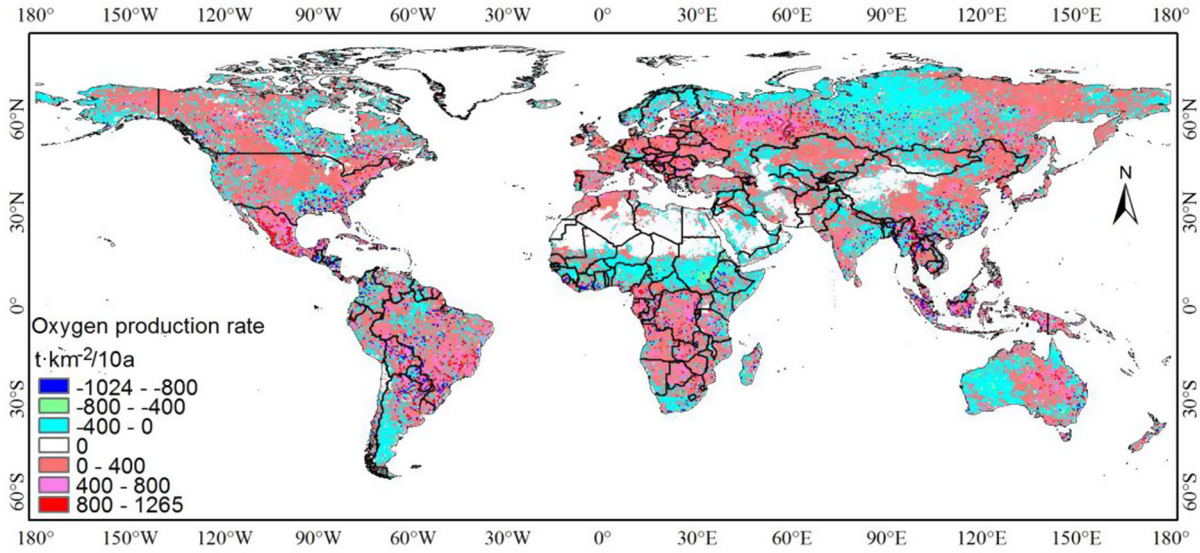

Fig. 5. Spatial distribution in oxygen production rate of global land vegetation over the period 2001–2010.

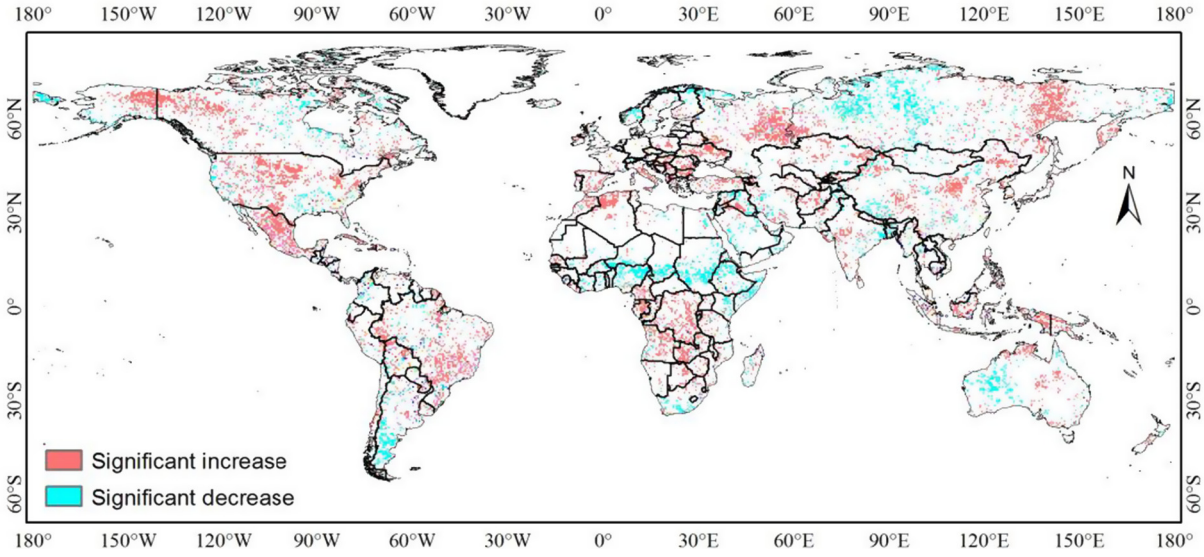

Fig. 6. Spatial distribution of significant changes in oxygen production of land vegetation over the period 2001–2010.

Table 5
Results of controlled experiments (10^9 t).

Controlled experiment	$O_{2,control}$	Actual analog value	$\Delta_{variation}$
Controlled experiment 1 (vegetation change)	194	192	2.08
Controlled experiment 2 (CO_2 concentration change)	199	192	7.61
Controlled experiment 3 (climate change)	191	192	−0.92

ranged between -500 t/km^2 and 0 t/km^2. Indeed, with the exception of Siberia and Alaska, which both experienced decreases, all other global regions saw increases in oxygen production (Fig. 8). Data show that climate change resulted in an increase, a decrease, or no change in oxygen production in 36.9%, 42.5%, and 20.6% of global area, respectively; this translates to a 1.15 times larger area of increase compared to decrease. Amounts of increase ranged between 0 t/km^2 and 500 t/km^2, and these areas were primarily distributed in the western and eastern parts of Russia, southern Africa, southern South America, western Canada, and Mexico. At the same time, decreasing amounts of oxygen production ranged between -500 t/km^2 and 0 t/km^2; areas that saw decreases were primarily distributed in western Siberia, northeastern China, southeastern China, Australia, India, the USA, and central Africa (Fig. 9).

In order to further analyze the factors influencing global areas that have seen distinct changes in oxygen production, Fig. 6 was overlapped with Figs. 7–9. This enabled data on vegetation, CO_2 concentration, and oxygen production changes due to climate change within each grid to be determined and compared. The maximum value in each case was deemed to be the most important factor explaining significant changes in oxygen production within the grid while the results of these comparisons enabled completion of Figs. 10 and 11. Data show that, overall, the factors influencing an increase in oxygen production within a particular region depend on its spatial location. In the Northern Hemisphere, for example, major factors were changes in vegetation and climate, while in the Southern Hemisphere, changes in CO_2 concentration were the major factor. Vegetation change was the major factor driving increases in oxygen production in mid-latitude regions of the Eurasian continent and North America, while climate change was the major influencing factor in high-latitude regions of the Northern Hemisphere. This variation turned out to also be the key influence

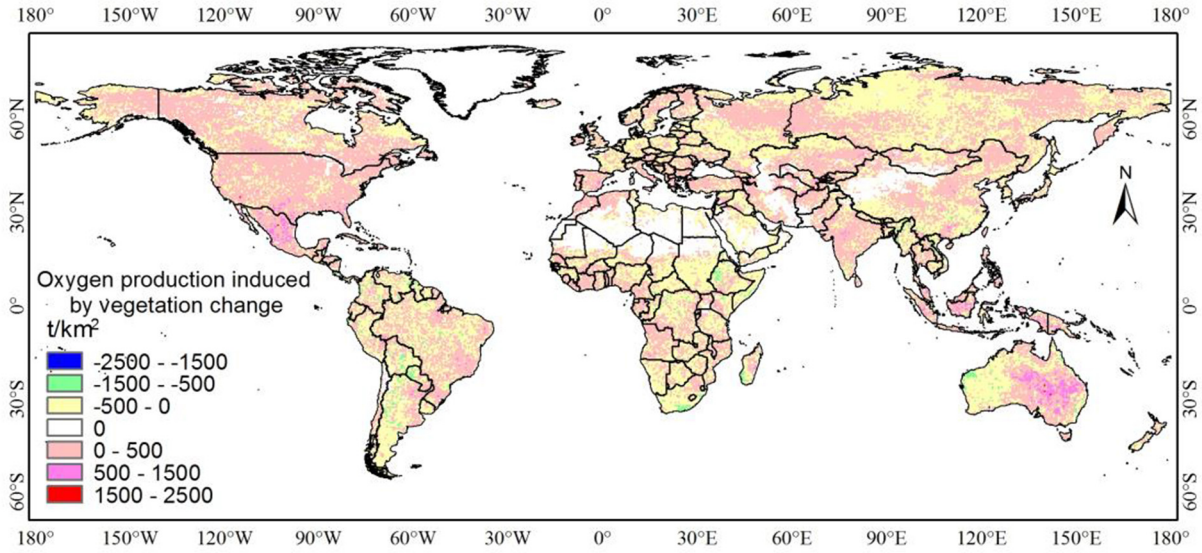

Fig. 7. Spatial distribution of oxygen production change induced by vegetation change.

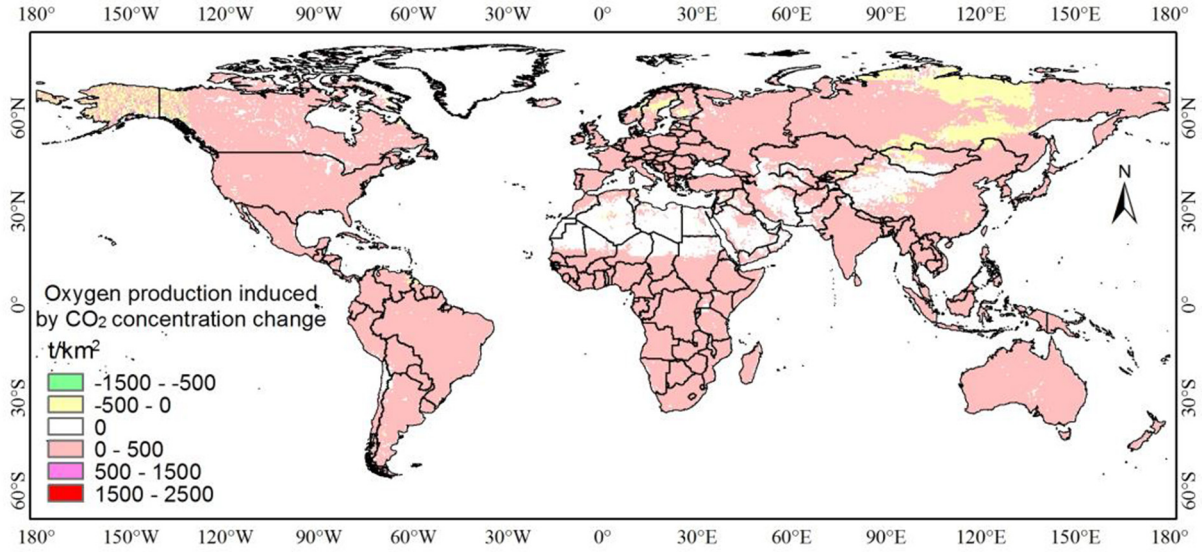

Fig. 8. Spatial distribution of oxygen production change induced by CO_2 concentration change.

underlying decreases in oxygen production in western Siberia and central Africa, while vegetation change was the major factor affecting production in western Australia and southern South America.

The major characteristics of vegetation change over time were extracted for regions that experienced significant increases or decreases in oxygen production (Table 6). Results show that the conversion of cultivated land and grassland into forested land was the main causative factor underlying significant oxygen production increases, while the conversion of forested land into cultivated areas was the main factor explaining significant decreases in the generation of this gas. The conversion of cultivated land into mixed or evergreen broad-leaved forests, as well as grassland into shrubs or evergreen broad-leaved forests, turned out to be the major changes underlying significant increases in global oxygen production. At the same time, the conversion of mixed and evergreen broad-leaved forests as well as shrubs into cultivated land, were the main changes responsible for significant reductions in oxygen production.

5. Discussion

The main contribution of this research is a simulation of global annual land vegetation oxygen production between 2001 and 2010. This is based on land vegetation productivity, the principles of plant photosynthesis and respiration, and the proportional relationship between oxygen and productivity. The results of this study clarify the fact that global annual oxygen production has tended to significantly increase over the last ten years in concert with climate warming, changes in global LUCC, and increasing air pollution. Research results show that vegetation-related oxygen production has changed significantly over almost 20.0% of the planet.

The light energy utilization coefficient (ε) expresses the proportional relationship between plant photosynthesis and the amount of C converted. This parameter is one of the driving forces of the C-FIX model; previous work has generally assumed this to be constant, with a value being 1.10 gC/MJ. However, because different plants utilize light energy in variable ways, a range of different ε values were utilized in this study, depending on global LUCC between 2001 and 2010. This is one significant area of improvement in this research when compared

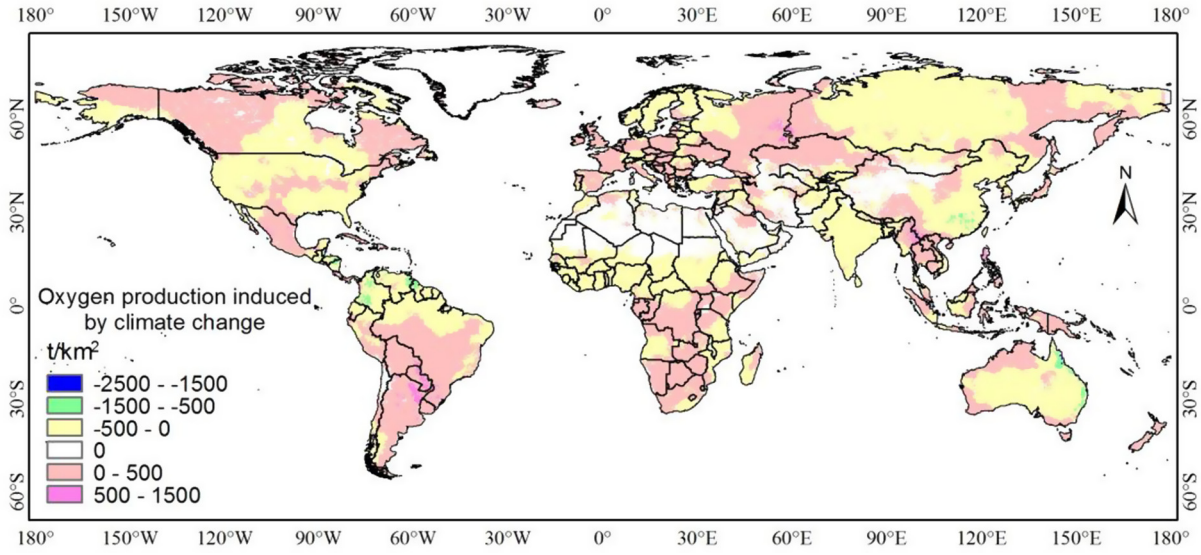

Fig. 9. Spatial distribution of oxygen production change induced by climate change.

with previous studies. Thus, to compare the effects of different ε values, global annual oxygen production for 2010 (264×10^9 t) was calculated using two values. Results show that if a ε value of 1.10 gC/MJ was used (i.e. the general literature-based value), global oxygen production was estimated to be 199×10^9 t and that a difference of 65.0×10^9 t between the two calculations was obtained. There are also spatial distributions between results, especially in South America and Africa (Fig. 12). In other words, the better the vegetation coverage in a region, the more obvious the difference; thus, improvements in the assignment of ε enhance the differentiation of oxygen production in different land use and land cover types, and increased the spatial heterogeneity of simulation results.

The estimation results of this study were verified by comparison with those from previous research, albeit limited to the same, or similar, time periods. This is important because limited research has been conducted to date that estimates global oxygen production using green plant productivity; most previous investigations in this area have emphasized NPP and NEP estimation, which vary for different plants and regions. Thus, NEP was converted into oxygen production in a 1:2.67 proportion, based on the principle of plant photosynthesis. The estimation results from this study can therefore be compared with previous data in the same way, by converting estimates for NPP and NEP into oxygen production. Data show that converted oxygen production estimates based on NPP are higher because this variable is elevated in nature compared to NEP. Thus, compared with existing research in this area, the values recovered by this analysis are relatively low, while close in terms of NEP to earlier studies. The conclusions presented here can therefore be considered reliable as they are close to those of earlier theoretical work (Table 7).

Many studies have emphasized the factors influencing changes in the C cycle in global terrestrial ecosystems. For instance, Potter et al. (2003) suggested that changes in CO_2 concentration have resulted from significant NEP increases in Eurasia, while Cao et al. (2005) noted that, in addition to changes in the proportion of this gas, climate change can also force an increase in global NEP. This was further corroborated by Peng and Dan (2016), who further clarified the fact that CO_2 is the most critical factor influencing the amplitude of variation and spatial distribution of global terrestrial NPP and NEP; indeed, these workers argued that the effects of this change are larger than those due to climate. This earlier study (Peng and Dan, 2016) utilized the CanESM2 model

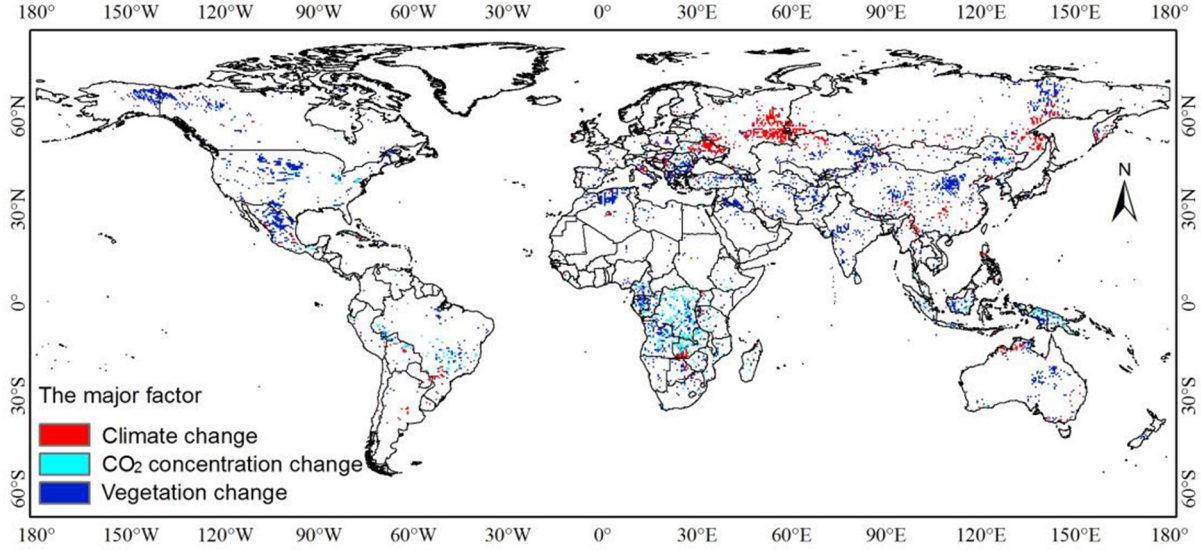

Fig. 10. The major factor affecting global oxygen production of land vegetation in regions with significant increases.

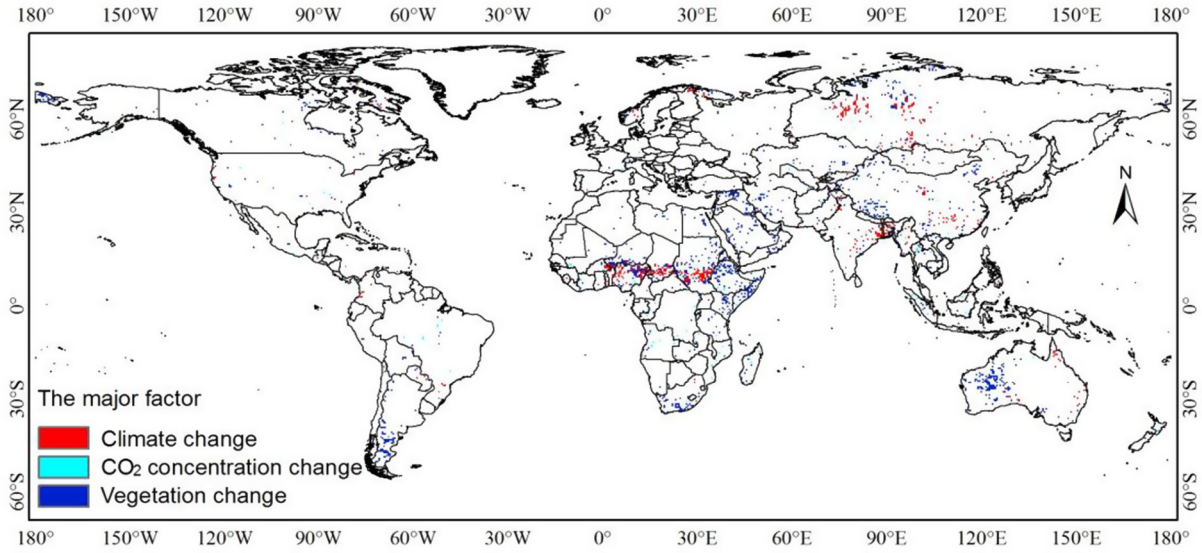

Fig. 11. The major factor affecting global oxygen production of land vegetation in regions with significant decreases.

and presented a quantitative analysis to explain how increasing CO_2 and changes due to climate change affect NEP. The results presented here have converged on the same conclusion, even though we transformed NEP to oxygen production. On this basis, a marked increase in CO_2 concentration gives rise to an increase (6.72×10^9 t) in vegetative oxygen production, while climate change leads to a concomitant reduction of about 3.88×10^9 t. The simulations presented in this paper suggest that increasing CO_2 concentrations lead to an increase of 7.61×10^9 t of vegetation oxygen production, while climatic change results in a 0.92×10^9 t reduction (Table 5). It is noteworthy that even though the two study periods are different, the results of this research are almost the same as those of Peng and Dan (2016).

The results of this study show that global annual oxygen production changed significantly around 2006. Prior to this date, global annual production had tended to slightly decrease, but subsequent to 2006, it significantly increased. Thus, to further explore the factors underlying the changes that took place at this time, time series correlations between global annual oxygen production and global vegetation NDVI were evaluated, as well as global average temperature and CO_2 concentration. The correlation coefficients for these comparisons are 0.37, −0.05, and 0.89, respectively, indicating that the changes in global oxygen production have been closely related to CO_2 concentration. Variance analyses were also performed on time series of global vegetation NDVI, average temperature, and CO_2 concentration, both before and after 2006. Results show extremely significant differences in CO_2 concentration before, and after this date ($P < 0.01$), while global vegetation NDVI and average temperature were not significant at these two time points. This result implies that changes in CO_2 concentration exerted a critical effect on changes in annual global oxygen production; thus, changes in the production of this gas before, and after 2006 are mainly the result of changes in CO_2 concentration.

The estimation results presented in this study elucidate the change tendencies of global vegetative oxygen production on the basis of the C-FIX model taking into consideration land use/cover and climate. At the same time, however, since the combustion of fossil fuels and animal and plant respiration also consume oxygen, green plants produce this gas via photosynthesis, and there are both horizontal and vertical movements and exchanges of air within the atmosphere, estimates for oxygen production might not be exactly the same as the actual spatial concentration distribution.

The simulation and estimation procedures utilized in this study also involved the complex processing of remote sensing images, including image mosaics and resetting, mask extraction, layer stacking, and grid calculations. These steps all mean that data extraction errors might have occurred in the transformation of coordinates, boundary line mosaics, and format conversions, and could influence the accuracy of results. It is therefore worth emphasizing that although the paper ignores NDVI values for non-vegetated areas, this index will still be influenced by elements such as atmospheric conditions, clouds, and the background plant canopy. It is therefore of considerable significance to ensure NDVI precision to achieve accurate simulation results.

There has been a marked increase in global oxygen production due to vegetation over the last ten years. The results of this study reveal the main factors that have influenced changes in the production of this gas via controlled experiments. Data show that changes in CO_2 concentration are the dominant factor controlling the global oxygen production,

Table 6
The main vegetation types in the dense regions with significant change in global oxygen production caused by vegetation change.

Dense regions with significant increases in oxygen production	Main vegetation conversion types causing oxygen production increase
Eastern Siberia	Conversion of shrubs into deciduous coniferous forests, from grassland into shrubs
Northeast China	Conversion of cultivated land into mixed forests or deciduous broad-leaved forests
Eastern Australia	Conversion of grassland into shrubs or evergreen broad-leaved forests
Mexico	Conversion of cultivated land into evergreen broad-leaved forests, from grassland into deciduous broad-leaved forests
North America	Conversion of cultivated land into evergreen coniferous forests, from grassland into shrubs
Alaska and Canada	Conversion of grassland into mixed forests or shrubs
Dense regions with significant decreases in oxygen production	Main vegetation conversion types causing oxygen production reduction
Western Australia	Conversion of evergreen broad-leaved forests into cultivated land, from shrubs into grassland
Southern tip of South America	Conversion of evergreen broad-leaved forests into deciduous coniferous forests, from shrubs into grassland
Eastern Africa	Conversion of mixed forests into cultivated land, from shrubs into cultivated land

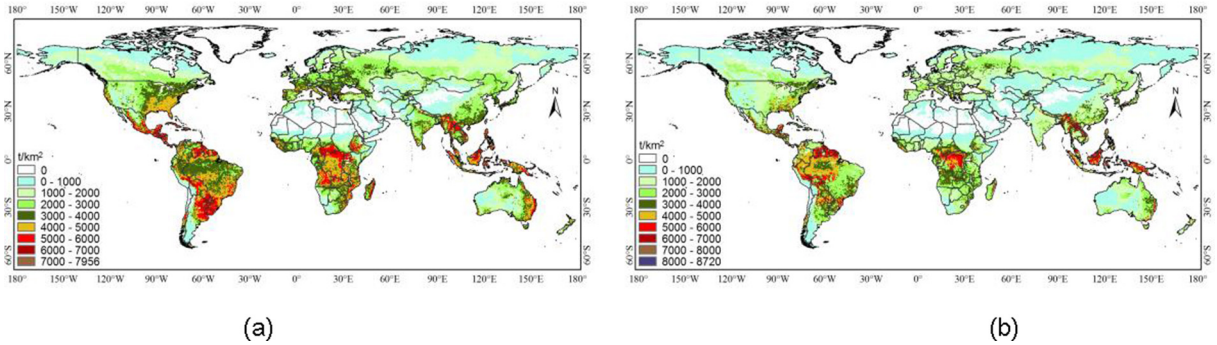

Fig. 12. Spatial distribution of global oxygen production of land vegetation in 2010 based on a constant of the light energy utilization ratio (a) and values of the light energy utilization ratio based on actual land use types (b).

at a 70.0% contribution rate, while vegetation (20.0%) and climatic change (10.0%) are much less significant. Changes in CO_2 concentration have led to increasing vegetation-related oxygen levels globally (Fig. 8), even though the production levels of this gas due to vegetation and climate changes have varied spatially. Data show that some areas have experienced positive changes, while others can be characterized in the opposite way, but both exert joint effects on the rate of contribution. This study also summarizes the oxygen production that has resulted from each element across all grids where changes are obvious, and accepts the one with a maximum value as the most important. The results of this study show that: 65.5% of grids that have exhibited obvious increases in oxygen production are the result of vegetation change, while 23.3% and 11.2% are due to climate change and CO_2 concentration, respectively. Similarly, 66.9% of grids that saw a reduction in oxygen production are the result of vegetation change, while 29.2% are due to climate, and 4.89% to CO_2 concentration. It can therefore be concluded that vegetation change is the dominant factor controlling changes in oxygen production at small scales. Further research on spatial variations will be required to determine the reasons that underlie changes in global oxygen production, including how differences in CO_2 concentration, vegetation, and climate influence the production of this key gas.

6. Conclusions

(1) The average global oxygen production of vegetation between 2001 and 2010 was 194×10^9 t, and the average annual rate of increase was 0.78×10^9 t/a. Data show that global oxygen production has tended to increase significantly over time, driven by concomitant increases in atmospheric CO_2 concentration and changes in vegetation. At the same time, climate change has tended to cause a decrease in global oxygen production, with increasing CO_2 concentration proving the most critical factor. Across 12.0% of the globe, oxygen production has significantly increased, while the opposite trend characterizes approximately 5.42% of land area. Regions that have experienced significant increases are primarily in eastern Siberia, eastern Europe, northeastern China, eastern Australia, southern Africa, eastern South America, Mexico, the central USA, and the border area between Alaska and Canada, while areas that have experienced significant decreases are primarily in western Siberia, central Africa, western Australia, and southern South America.

(2) Annual oxygen production in South America between 2001 and 2010 was the highest globally, accounting for approximately 28.0% of the total, and production on all continents has tended to increase. In particular, oxygen production in Asia, North America, and Europe has significantly increased, while in Africa, South America, and Oceania this trend has been only slight.

(3) Results show that changes in vegetation and climate were the major factors driving significant increases in oxygen production across the Northern Hemisphere, while changes in CO_2 concentration can mainly explain the significant increase in the Southern Hemisphere. In terms of particular changes in vegetation, conversions of cultivated land and grassland to forested land have been the main factor underlying increases in global oxygen production, while the conversion of forested land to cultivated land is the main reason for decreases.

(4) Data show that the spatial distribution of global annual oxygen

Table 7
Comparison of the results of this study with those of previous studies.

No.	Previous research results					The results of this study
	Reference	Method	Simulated vegetation	Simulated index	Transformed oxygen amount	
1	Jiang et al. (2011)	AVIM2 model	Global terrestrial ecosystems	NPP	14.3 t/hm^2 (2001–2004)	14.2 t/hm^2 (2001–2004, Global)
2	Jiao et al. (2014)	Miami model	Global forest ecosystems	NPP	Asia 17.3 t/hm^2 Europe 17.4 t/hm^2 North America 15.7 t/hm^2 (1961–2008)	Asia 10.6 t/hm^2 Europe 14.9 t/hm^2 North America 9.59 t/hm^2 (2001–2010, Global)
3	Liu (2001)	TEPC model	Terrestrial ecosystems in China	NPP	13.1 t/hm^2 (1993–1999)	10.8 t/hm^2 (2001, China)
4	Cao et al. (2005)	CEVSA model	Global terrestrial ecosystems	NEP	10.2 t/hm^2 (1981–2000)	14.2 t/hm^2 (2001, Global)
5	Churkina et al. (2003)	BIOME-BGC model	Coniferous forests in Europe	NEP	19.6 t/hm^2 (1952–1998)	14.4 t/hm^2 (2001, Coniferous forests in Europe)
6	Zhang et al. (2014)	C-FIX model	Forests in Heilongjiang Province	Oxygen production	8.51 t/hm^2 (2009)	10.3 t/hm^2 (2009, forests in Heilongjiang Province)
7	Warnant et al. (1994)	CARAIB mode	Global terrestrial ecosystems	NPP	Oxygen production tended to decrease with increasing latitude, and it was higher in tropical areas	Oxygen production tended to decrease with increasing latitude, and it was higher in tropical areas

production between 2001 and 2010 is highly consistent, as gas generation has tended to decrease from the equator to the poles. A higher level of oxygen production characterizes tropical areas, and consistently high levels are mainly seen in Southeast Asia, central Africa, southern North America, and northern South America.

Acknowledgments

Financial support for this study was provided by the National Natural Science Foundation of China (Grant Nos. 41771067, 41571199).

References

Cao, M., Prince, S.D., Tao, B., Small, J., Li, K., 2005. Regional pattern and interannual variations in global terrestrial carbon uptake in response to changes in climate and atmospheric CO_2. Tellus Ser. B 57 (3), 210–217.
Chen, B., Lu, S., 2009. Valuing ecological services of green space of West Lake scenic area in Hangzhou. J. Zhejiang Univ. Agric. Life Sci. 35 (6), 686–690.
Chen, B., Wang, S.Q., Liu, R.G., Song, T., 2007. Study on modeling and spatial patterns of net primary production in China's terrestrial ecosystem. Resour. Sci. 29 (6), 45–53.
Churkina, G., Tenhunen, J., Thornton, P., Falge, E.M., Elbers, J.A., Erhard, M., Grünwald, T., Kowalski, A.S., Rannik, U., Sprinz, D., 2003. Analyzing the ecosystem carbon dynamics of four European coniferous forests using a biogeochemistry model. Ecosystem 6 (2), 168–184.
Foley, J.A., Defries, R., Asner, G.P., Barford, C., Bonan, G., Carpenter, S.R., Chapin, F.S., Coe, M.T., Daily, G.C., Gibbs, H.K., Helkowski, J.H., Holloway, T., Howard, E.A., Kucharik, C.J., Monfreda, C., Patz, J.A., Prentice, C., Ramankutty, N., Snyder, P.K., 2005. Global consequences of land use. Science 309 (22), 570–573.
Friedl, M.A., Sulla-Menashe, D., Tan, B., Schneider, A., Ramankutty, N., Sibley, A., Huang, X.M., 2010. MODIS collection 5 global land cover: algorithm refinements and characterization of new datasets. Remote Sensing Environ. 114 (1), 168–182.
Grimm, N.B., Faeth, S.H., Golubiewski, N.E., Redman, C.L., Wu, J.G., Bai, X.M., Briggs, J.M., 2008. Global change and the ecology of cities. Science 319 (8), 756–760.
Hansen, M.C., Potapov, P.V., Moore, R., Hancher, M., Turubanova, S.A., Tyukavina, A., Thau, D., Stehman, S.V., Goetz, S.J., Loveland, T.R., Kommareddy, A., Egorov, A.V., Chini, L., Justice, C.O., Townshend, J.R.G., 2013. High-resolution global maps of 21st century forest cover change. Science 342 (15), 850–853.
IPCC, 2013. Climate change 2013: The Physical Science Basis, Contribution of Working Group I to the Fifth Assessment Report of the Intergovernmental Panel on Climate Change. Cambridge University Press, Cambridge, UK and New York, USA.
Jacobsen, D., 2008. Low oxygen pressure as a driving factor for the altitudinal decline in taxon richness of stream macroinvertebrates. Commun. Ecol. 154 (4), 795–807.
Jiang, C., Xu, Y.F., Ji, J.J., Li, Y.C., 2011. Influences of the decadal variation of ENSO on the carbon flux in the terrestrial ecosystems. Earth Sci. Front. 18 (6), 107–116.
Jiao, C.C., Yu, G.R., Zhan, X.Y., Zhu, X.J., Chen, Z., 2014. Spatial pattern and regional characteristics of global forest ecosystem net primary productivity. Q. Sci. 34 (4), 699–709.
Kasting, J.F., Siefert, J.L., 2002. Life and the evolution of Earth's atmosphere. Science 296 (5570), 1066–1068.
Kimball, H.H., 1928. Amount of solar radiation that reaches the surface of the earth on the land and on the sea, and methods by which it is measured. Mon. Weather Rev. 56 (10), 393–398.
Lenton, T.M., 2003. The coupled evolution of life and atmospheric oxygen. Evol. Planet Earth 35–53.
Liu, M.L., 2001. Land-use/land-cover change and terrestrial ecosystem phytomass carbon pool and production in China. Chin. Acad. Sci. 1–2.
Liu, X.X., Zhang, L.J., Li, W.L., Zhang, X.Z., Jiang, C.Y., 2015. Simulating the changing oxygen production of terrestrial vegetation and its influencing factors in China. Acta Ecol. Sin. 35 (13), 4314–4325.
Lu, L., Li, X., Veroustraete, F., 2005. Terrestrial net primary productivity and its spatial-temporal variability in western China. Acta Ecol. Sin. 25 (5), 1026–1032.
Lu, L., Li, X.P., Veroustraete, F., Dong, Q.H., 2004. Estimation of NPP in Western China using remote sensing and the C-Fix model. Proc. IEEE 1, 7803–8743.
Ma, J.Y., Yin, K., Lin, T., 2011. Analysis of the carbon and oxygen balance of a complex urban ecosystem: a case study in the coastal city of Xiamen. Acta Sci. Circumstantiae 31 (8), 1808–1816.
Peng, J., Dan, L., 2016. The 100-year scale response of terrestrial ecosystem carbon fluxes to climate-carbon cycle caused by increasing atmospheric CO_2 concentration using an Earth System Model. Acta Ecol. Sin. 36 (21), 6939–6950.
Peng, J.Y., 2003. Roles of vegetation on balance of carbon and oxygen in the Pearl River Delta. Acta Sci. Nat. Univ. Sunyatseni 42 (5), 105–108.
Peng, X.L., Guo, Z.H., Wang, B.S., 2000. Use of GIS and RS to estimate the light utilization efficiency of the vegetation in Guangdong, China. Acta Ecol. Sin. 20 (6), 903–909.
Potter, C., Klooster, S., Myneni, R., Genovese, V., Tan, P.N., Kumar, V., 2003. Continental-scale comparisons of terrestrial carbon sinks estimated from satellite data and ecosystem modeling 1982–1998. Global Planet. Change 39 (3–4), 201–213.
Running, S.W., Thornton, P.E., Nemani, R., Glassy, J.M., 2000. Global terrestrial gross and net primary productivity from the earth observing system. Methods Ecosyst. Sci. 44–57.
Santilli, R.M., 2000. Alarming oxygen depletion caused by hydrogen combustion and fuel cells and their resolution by magnegas. In: International Hydrogen Energy Forum 2000, Munich, Germany.
Schäfer, G., 2004. How did the earth's oxygen atmosphere originate? Anästhesiol. Intensivmed. Notfallmed. Schmerzther. 39, 19–27.
Semenza, G.L., 2001. Hypoxia-inducible factor 1: Oxygen homeostasis and disease pathophysiology. Trends Mol. Med. 7 (8), 345–350.
Tao, B., Ge, Q.S., Li, K.R., Shao, X.M., 2001. Progress in the studies on carbon cycle in terrestrial ecosystem. Geogr. Res. 20 (5), 564–575.
Tsegaye, D., Moe, S.R., Vedeld, P., Aynekulu, E., 2010. Land-use/cover dynamics in Northern Afar rangelands, Ethiopia. Agric. Ecosyst. Environ. 139, 174–180.
Veroustraete, F., Sabbe, H., Eerens, H., 2002. Estimation of carbon mass fluxes over Europe using the C-FIX model and Euroflux data. Remote Sensing Environ. 83 (3), 376–399.
Verstraeten, W.W., Veroustraete, F., Feyen, J., 2006. On temperature and water limitation of net ecosystem productivity: implementation in the C-Fix model. Ecol. Model. 199 (1), 4–22.
Viera, A.J., Garrett, J.M., 2005. Understanding interobserver agreement: the kappa statistic. Fam. Med. 37 (5), 360–363.
Warnant, P., François, L., Strivay, D., Gerard, J.C., 1994. CARAIB: a global model of terrestrial biological productivity. Global Biogeochem. Cycl. 8 (3), 255–270.
Zak, M.A., Cabido, M., Cáceres, D., Díaz, S., 2008. What drives accelerated land cover change in central Argentina? Synergistic consequences of climatic, socioeconomic and technological factors. Environ. Manage. 42 (2), 181–189.
Zhang, D.Y., Feng, Z.K., Li, Y.Q., Zhang, L.J., Dong, B., 2011. Remote sensing estimation of forest net primary productivity in Heilongjiang Province with C-FIX Model. Sci. Silvae Sin. 47 (7), 13–19.
Zhang, L.J., Jiang, C.Y., Ma, J., Zhang, A.K., Jiang, L.Q., Wu, S., 2014. Forest change and its impact on the quantity of oxygen release in Heilongjiang Province during the Past Century. Acta Ecol. Sin. 34 (2), 430–441.
Zhang, Y., Wang, Q., Li, B.J., Wang, W.M., 2007. Study on forecasting ecological land demand with carbon-oxygen balance method. China Land Sci. 21 (6), 23–28.
Zhou, S.Z., Zhang, R.Y., Zhang, C., 2003. Meteorology and Climatology. Higher Education Press, Beijing.
Zhu, W.Q., Chen, Y.H., Pan, Y.Z., Li, J., 2004. Estimation of light utilization efficiency of vegetation in China based on GIS and RS. Geomatics Inf. Sci. Wuhan Univ. 29 (8), 694–698.
Zhu, W.Q., Pan, Y.Z., He, H., Yu, D.Y., 2006. Simulation of maximum light use efficiency for some typical vegetation types in China. Acta Ecol. Sin. 51 (4), 457–463.